Decoupling of large-scale brain networks supports the consolidation of durable episodic memories

Markus H Sneve[1], Håkon Grydeland[1] , Inge K Amlien[1], Espen Langnes[1], Kristine B Walhovd[1,2], Anders M Fjell[1,2]

[1] Center for Lifespan Changes in Brain and Cognition, Department of Psychology, University of Oslo, Norway

[2] Department of Physical medicine and rehabilitation, Unit of neuropsychology, Oslo University Hospital, Norway

Address correspondence to:

Markus Handal Sneve

Dept. of Psychology

Pb. 1094 Blindern, 0317 Oslo, Norway

Phone: +47 22 84 52 16

Fax: +47 22 84 50 01

E-mail: m.h.sneve@psykologi.uio.no

Keywords

Long-term memory

Consolidation

Subsequent memory

FMRI

Functional connectivity

Hippocampus

Abstract

At a large scale, the human brain is organized into modules of interconnected regions, some of which play opposing roles in supporting cognition. In particular, the Default-Mode Network (DMN) has been linked to operations on internal representations, while task-positive networks are recruited during interactions with the external world. Here, we test the hypothesis that the generation of durable long-term memories depends on optimal recruitment of such antagonistic large-scale networks. As long-term memory consolidation is a process ongoing for days and weeks after an experience, we propose that individuals characterized by strong decoupling of the DMN and task-positive networks at rest operate in a mode beneficial for the long-term stabilization of episodic memories. To capture network connectivity unaffected by transient task demands and representative of brain behavior outside an experimental setting, 87 participants were scanned during rest before performing an associative encoding task. To link individual resting-state functional connectivity patterns to time-dependent memory consolidation processes, participants were given an unannounced memory test, either after a brief interval or after a retention period of ~6 weeks. We found that participants with a resting state characterized by high synchronicity in a DMN-centered network system and low synchronicity between task-positive networks showed superior recollection weeks after encoding. These relationships were not observed for information probed only hours after encoding. Furthermore, the two network systems were found to be anticorrelated. Our results suggest that this memory-relevant antagonism between DMN and task-positive networks is maintained through complex regulatory interactions between the systems.

1. Introduction

Episodic long-term memory consolidation is a process that progresses over time, starting immediately following the encoding of an event and continuing through days and nights, months and possibly years (Dudai et al., 2015). Recent efforts in human neuroimaging have shed light on brain processes during the initial post-encoding interval that are relevant for early consolidation and subsequent memory performance, either by investigating post-stimulus activity time-locked to the offset of encoding events (Ben-Yakov et al., 2014, 2013; Ben-Yakov and Dudai, 2011), or intrinsic network activity during post-encoding rest periods (Schlichting and Preston, 2014; Stevens et al., 2010; Tambini et al., 2010; Tambini and Davachi, 2013; van Kesteren et al., 2010). These studies have elegantly demonstrated that the representational state of memory traces immediately following encoding is linked to retrieval success after short periods of retention.

There is a however also a strong consensus that systems consolidation – i.e. the transformation of labile representations into enduring *long-term* memories (Nadel and Moscovitch, 1997; Squire and Alvarez, 1995) – depends on repeated replay, and thus strengthening, of internal representations over extended periods of time, involving periods of sleep (Diekelmann and Born, 2010; Stickgold, 2013). On a neuronal level, this repeated accessing of labile representations is suggested to occur through recurrent communication during sleep and awake rest between the hippocampus and neocortical networks (Dudai et al., 2015). Much evidence show that such neocortical networks can exist in antagonistic relationships: introspection and the recruitment of networks involved in internally oriented cognition suppresses networks supporting interactions with external representations, and vice versa (Daselaar et al., 2009; Kim, 2011; Raichle et al., 2001). Efficient decoupling between the brain systems recruited during the two attentional modes – internal mentation and operations on external stimuli – has been

associated with optimal behavioral performance on a variety of tasks (Eichele et al., 2008; Fox et al., 2005; Kelly et al., 2008). Thus, an intriguing hypothesis is that the prolonged accessing of internal representations – thought to underlie successful systems consolidation – is supported by the combined up- and down-regulation of antagonistic neocortical systems.

A strong neocortical candidate for long-term memory-relevant processing is the Default-Mode Network (DMN), as it is closely connected to the medial temporal lobes (MTL; Buckner et al., 2008) and is functionally coupled to processes involved in attention to internal representations (Andrews-Hanna et al., 2014; Konishi et al., 2015; Smallwood et al., 2013; Spreng et al., 2014). Moreover, the retrieval of remote memories recruits DMN nodes more strongly than does retrieval of information encoded the same day (Frankland and Bontempi, 2005; Gais et al., 2007; Takashima et al., 2007; Wiltgen et al., 2004), suggesting that DMN regions are particularly central in accessing information after prolonged retention intervals. The DMN is commonly found to be decoupled with sensory and perceptual brain regions (Sadaghiani et al., 2015; Schooler et al., 2011), as well as the external attention system (EAS) consisting of several task-positive networks including the dorsal attention, the cingulo-opercular, and the fronto-parietal network (Anticevic et al., 2012; Fox et al., 2005). From this, we would expect that individuals recruiting the DMN while at the same time disengaging task-positive networks operate in a mode beneficial for the long-term stabilization of episodic memories.

In the present study, using functional magnetic resonance imaging (fMRI) and an individual differences approach, we investigate how brain network communication may support the formation of durable long-term memories. Rather than focusing on post-encoding rest periods that reflect state-dependent brain processes likely active only until a new encoding situation is encountered, we aimed at capturing task-independent network interactions reflective of the brain's default behavior outside an experimental

setting. We therefore measured rsFC *pre*-encoding, i.e. before two groups of participants performed an associative encoding task followed by an unannounced memory test. For one group, we estimated episodic memory capacity over commonly used short retention intervals (hours) between encoding and test. Crucially, to investigate associations between brain network interactions and capacity to form durable long-term memories, we used a delay interval of several weeks in the second group of participants. As the effect of encoding and retrieval processes on performance should be unaffected by manipulations of retention intervals, this made it possible to separate connectivity patterns enabling efficient consolidation from encoding and retrieval influences.

2. Materials and Methods

2.1. Participants

Eighty-nine participants (female n = 60; age range 19.5 – 38.6; mean age 25.4) gave written informed consent and took part in the study, which was approved by the Regional Ethical Committee of South Norway. Participants reported no history of neurological or psychiatric disorders, chronic illness, premature birth, learning disabilities, or use of medicines known to affect nervous system functioning. They were further required to be right-handed, speak Norwegian fluently and have normal or corrected to normal hearing and vision. Moreover, participants were required to score ≥26 on the Mini Mental State Examination (Folstein et al., 1975), and have a Beck Depression Inventory (Beck and Steer, 1987) score ≤16. At scanning a separate clinical sequence (T2-FLAIR) was included for neuroradiological evaluation by a neuroradiologist, and the scans were required to be deemed free of significant injuries or conditions. One person was excluded due to an incidental MRI finding, and one due to excessive motion (>1.5 mm) during the resting state fMRI (rsfMRI) scan. Participant demographics are summarized in Table 1.

--- INSERT TABLE 1 ABOUT HERE ---

2.2. Experimental design

Participants were scanned at rest (eyes closed) using BOLD fMRI before going through two fMRI runs of an incidental memory-encoding task. Participants were explained the task verbally and did not go through any practice session before entering the scanner. All participants reported staying awake throughout the scan. For 50 participants (short delay group) an fMRI test session followed 1.5 hours after the last encoding trial. The

remaining 37 participants (long delay group) were given the memory test when returning for neuropsychological testing after on average ~6.5 weeks.

The memory task was optimized to allow for the investigation of individual differences in source memory performance, i.e., the ability to remember a previously encountered item together with information about the encoding context. In line with recent theoretical accounts of source memory, our conceptualization of source memory considers all retained information about the encoding context as relevant, not only information about time and space (e.g., Ranganath and Ritchey, 2012). During encoding participants went through 100 trials of a task in which they performed simple evaluations of everyday objects and items (Figure 1A). A trial had the following structure: a black and white line drawing of an object was presented on the screen while a female voice asked either "Can you eat it?" or "Can you lift it?" Both questions were asked equally often and were pseudorandomly mixed across the different objects. Participants were instructed to produce yes/no-responses based on their subjective evaluations of object/task-contingencies, and that there were no correct responses to the task. Importantly, participants did not know that they were part of a memory experiment and would be tested on the evaluated material, and remained ignorant about this until just before the test session.

--- INSERT FIGURE 1 ABOUT HERE ---

During test, 200 line drawings of objects were presented; 100 of these had been shown and evaluated during encoding while the remaining 100 objects were new (Figure 1B). A test trial started with the presentation of an object (old or new, pseudorandomly picked) and the question "Have you seen this item before?" Participants were instructed to respond "Yes" if they remembered seeing the item during the encoding phase, and "No" otherwise. If the participant indicated that (s)he remembered seeing the object, a new question followed: "Can you remember what you were asked to do with the item?"

A “Yes”-response to this question, indicating that the participant also remembered the action associated with the object during encoding, led to a final control question: “Were you asked to eat it or lift it?” Here, the participant indicated either “Eat” ("I evaluated whether I could eat the item during the encoding phase)" or “Lift” ("I evaluated lifting the item"). Note that the specific questions asked during scanning were simplified to fit within the temporal limits of the paradigm, but that all participants were instructed in detail before the test session that the questions pertained to the item-action evaluation performed at encoding. The task has also been described in Sneve et al. (2015).

A participant’s raw source memory score was calculated as the percentage of encoded items that were recognized with correct recollection of the associated encoding action. Thus, participants had to correctly recognize an item (correct “Yes” response to test question 1), state that they remembered the associated action (“Yes” response to test question 2), and explicitly pick the correct associated action (correct response to question 3) for that item to fall into the raw source memory category. A corrected source memory score was calculated from the raw source memory score by subtracting the number of times a participant produced a wrong source response (i.e., wrong response to test question 3). Here we assumed that guessing behavior would produce correct/incorrect responses equally often. All main analyses were run on the corrected source memory estimates, but results using raw source memory estimates produced similar results and are reported in the Supplementary Material.

Signal detection theory was used to investigate potential differences in response criteria (C) between the two groups, i.e. differences in the tendency to characterize a stimulus as new or old as a factor of retention interval (Stanislaw and Todorov, 1999). The majority of the participants (see Supplementary Table 1) were also tested on three subtests of the Wechslers Adult Intelligence Scale (WASI; Wechsler, 1999): Vocabulary, Matrix Reasoning, and Digit Span. Individual Vocabulary and Matrix Reasoning scores were t-

standardized before being used as covariates in control analyses, representing central aspects of full scale IQ. Individual forward and backward Digit Span results were summed into one score per participant, representing working memory performance.

2.3. MRI scanning

Imaging was performed at a Siemens Skyra 3T MRI unit with a 24-channel head coil. For the rsfMRI scan, 43 slices (transversal, no gap) were measured using T2* BOLD EPI (TR=2390ms; TE=30ms; flip angle=90°; voxel size=3x3x3mm; FOV=224x224; interleaved acquisition; GRAPPA=2). The rsfMRI run produced 150 volumes and lasted ~6 minutes which has been shown to be sufficient to produce stable connectivity measures (Van Dijk et al., 2010). Three dummy volumes were collected at the start of the rsfMRI scan to avoid T1 saturation effects in the analyzed data. Additionally, a standard double-echo gradient-echo field map sequence was acquired for distortion correction of the EPI images. Anatomical T1-weighted MPRAGE images consisting of 176 sagittally oriented slices were obtained using a turbo field echo pulse sequence (TR = 2300 msec, TE = 2.98 msec, flip angle = 8°, voxel size = 1 × 1 × 1 mm, FOV= 256 × 256 mm).

2.4. Pre-processing and parcellation of MRI data

Cortical reconstruction and volumetric segmentation of the T1-weighted scans were performed with Freesurfer 5.3. This processing included segmentation of the subcortical white matter and deep grey matter volumetric structures (including the hippocampus) (Fischl et al., 2004a, 2002), surface inflation (Fischl et al., 1999a), registration to a spherical atlas which utilized individual cortical folding patterns to match cortical geometry across subjects (Fischl et al., 1999b), and parcellation of the cerebral cortex into units based on gyral and sulcal structure (Desikan et al., 2006; Fischl et al., 2004b).

RsfMRI-data were corrected for B0 inhomogeneity, motion and slice timing corrected, and smoothed (5mm FWHM) in volume space using FSL (http://fsl.fmrib.ox.ac.uk/fsl/fslwiki). Next, FMRIB's ICA-based Xnoiseifier (FIX; Salimi-Khorshidi et al., 2014) was used to auto-classify noise components and remove them from the rsfMRI data. The classifier was trained on a scanner-specific dataset in which resting state fMRI data from 16 participants had been manually classified into signal and noise components (age span in training set: 18-40; fMRI acquisition parameters identical to the current study). Such ICA-based procedure for denoising fMRI data has been shown to effectively reduce motion-induced variability, outperforming methods based on removing motion spikes in the dataset (Pruim et al., 2015). Motion confounds (24 parameters) were regressed out of the data as a part of the FIX routines. Freesurfer-defined individually estimated anatomical masks of cerebral white matter (WM) and cerebrospinal fluid / lateral ventricles (CSF) were resampled to each individual's functional space. All $1mm^3$ anatomical voxels that "constituted" a $27mm^3$ functional voxel had to be labeled as WM or CSF for that functional voxel to be considered a functional representation of non-cortical tissue. Following FIX, average time series were extracted from functional WM- and CSF-voxels, and were regressed out of the FIX-cleaned 4D volume. Following recent recommendations about noise removal from resting-state data (Hallquist et al., 2013) we band-pass filtered the data (.009 - .08Hz) after regression of confound variables.

--- INSERT FIGURE 2 ABOUT HERE ---

In analyzing the rsfMRI data, we took advantage of Yeo and colleagues' (Yeo et al., 2011) cortical parcellation estimated by intrinsic functional connectivity from 1000 participants and made available in Freesurfer's average surface space. Details about the networks are presented in Figure 2A. The parcellation scheme consisted of 17 bilateral networks as well as values representing the estimated confidence of each surface vertex

belonging to its assigned network. Typically, network assignments were less confident for vertices close to the boundaries between two networks (Yeo et al., 2011). The 17-network parcellation and the associated confidence map, estimated from 1000 participants, were resampled into each participant's surface space using the intersubject registration created during Freesurfer's cortical reconstruction steps. The individualized parcellation/confidence maps were then converted into functional volume space using a projection factor of 0.5 from the estimated white/gray matter boundary (i.e., half way into the cortical sheet). This step ensured that only gray matter dominated voxels were included in the volumetric representations of the networks. Each network and its confidence map were thus brought from the surface (vertex) level to the volume (voxel) level. Next, in volume space and in a voxel-wise fashion, we extracted pre-processed rsfMRI time series data from all 17 networks, and from a region of interest representing the two hippocampi. Finally, we estimated connectivity between- and within all networks, resulting in an 18x18 network connectivity matrix per participant (see Figure 2B for a representation of this matrix averaged across all participants). Between-network connectivity was calculated as the average Fisher z-transformed correlation (Silver and Dunlap, 1987) between all voxels in two networks weighted by the product of each pair of voxels' normalized confidence values. The normalization involved rescaling of confidence values to fall between 0 (lowest confidence) and 1 (highest confidence) within a network, ensuring that differences in scaling of the confidence values between networks did not influence weighting in favor of high-confidence networks (Yeo et al., 2011). To summarize: if network A consisted of N voxels and network B consisted of M voxels, correlations were calculated across all NxM voxel combinations. The resulting NxM correlation map was then weighted by an NxM confidence map, ensuring that voxels strongly associated with their respective networks contributed the most to the connectivity estimates. Within-network connectivity was calculated following the same steps, and reflected average connectivity

within a network. When investigating hippocampal connectivity, all hippocampal voxels were equally weighted in the calculations.

Temporal signal-to-noise ratios (tSNR) were calculated for all 17 networks and the hippocampus. As expected, the Limbic networks (NW9 and NW10) showed lower tSNR than the other networks due to their proximity to air-tissue boundaries. However, all tSNR values in all networks for all participants were within or above the ranges reported in similar regions by authoritative studies (e.g., Yeo et al., 2011; see Supplementary Figure 1).

2.5. Connectivity analyses

To investigate relationships between cortical brain network connectivity and source memory performance, we first standardized each participant's 18x18 network connectivity matrix using Matlab's *zscore*-function. This involved converting "raw" Fisher-transformed connectivity values into standard deviation units above or below the mean connectivity of the 171 unique edges in the matrix, and allowed comparisons across participants independent of individual differences in absolute connectivity levels (see Figure 2C for average representations of these matrices in the two groups; Supplementary Figure 2 for a representation of differences in absolute connectivity levels). Such standardization of individual connectivity measures is commonly used to minimize the influence of nuisance variables known to affect individuals' average connectivity levels (Yan et al., 2013). The values shown in Figure 2C should thus be interpreted as connectivity relative to individuals' global connectivity levels, that is, negative values indicate reduced connectivity relative to participant baseline and not negative correlations/anticorrelations. Next, relationships between standardized rsFC and source memory performance were calculated separately for the long and short-term memory groups using Spearman's *rho*, producing 18x18 matrices of correlation coefficients and their associated *p*-values. Significant between-group differences in

correlation coefficients were established following Fisher's r-to-z-transformation (shown to be valid for Spearman's *rho* by Myers and Sirois, 2006).

To control for multiple comparisons, we used random permutation testing in combination with cluster-based statistics, as described in (Han et al., 2013). The method is an extension of the Network-based Statistics method (NBS; Zalesky et al., 2010), and has been optimized to identify clusters of connected edges in brain connectivity graphs that are significantly correlated with behavioral measures. As NBS clusters form in topological and not physical space, the specific network arrangement in the connectivity matrix does not affect cluster properties. For each group and for positive/negative correlations separately, we established the extent of clusters of connected edges at an uncorrected threshold of $p<.05$. This corresponded to a correlation coefficient stronger than *rho* ±.28 in the short delay group and *rho* ±.325 in the long delay group. Next, we repeated the procedure 10.000 times per group, randomly permuting the behavioral data while keeping the connectivity data stationary (i.e., in adherence with the exchangeability criterion in permutation testing (Nichols and Holmes, 2002)). Finally, significance levels of clusters identified in the empirical data were estimated from the permuted null distribution of cluster extents. A significant effect indicated that a cluster of connected significant correlations was larger than expected due to chance at the family-wise error corrected $p<0.05$ level, however not that any specific individual correlation was significant. This latter aspect, significant corrected single-edge correlations, was investigated by comparing the observed relationships to the 95th percentile of the permuted distribution of single-edge correlation coefficients.

In additional analyses, we used alternative cluster-forming thresholds: $p < .01$ (short delay group *rho* ±.36, long delay group *rho* ±.42), and $p < .005$ (short delay group *rho* ±.39, long delay group *rho* ±.45; see Supplementary Figure 4).

3. Results

3.1. Subsequent memory performance after short and long delays

In the short delay group, on average 50.4% (range 24%-90%; SD 15.6%) of the encoded item-action associations were remembered with source information following correction for wrong recollection responses. Unsurprisingly, the long delay group remembered less (mean corrected source memory: 8.7%; range -3%-28%; SD 7.5%), but at the group level still retained significant amounts ($p < 10^{-7}$) of relevant information throughout the delay period (Supplementary Table 1). Analyses on the signal detection theory response criterion C showed that there were no significant differences between the groups ($p = .69$) in the propensity to report recognition of the test item ("yes"-response to Test question 1), and that both the short delay group ($C=.52$) and the long delay group ($C=.47$) were slightly conservative ($C>0$, $p<10^{-6}$) in their recognition judgments.

--- INSERT FIGURE 3 ABOUT HERE ---

3.2. Relationship between rsFC and source memory capacity after short and long delays

Following standardization of each participant's connectivity matrix, we correlated individual differences in within- and between-network connectivity with source memory performance. Correlation coefficients across the entire 18x18 connectivity matrix are shown for the two groups in Figure 3A. At a single-edge level, one edge in the long delay group survived correction for multiple comparisons through permutation: pre-encoding connectivity between the Parietal Memory Network (NW 11) and a subnetwork of the DMN (NW 15) correlated strongly and positively with source memory capacity after retention intervals of weeks (*rho* = .56; uncorrected $p < .0003$). No edges survived single-edge correction in the short delay group.

Figure 3B shows the correlation matrices thresholded at the cluster-forming threshold ($p < 0.05$). Permutation testing was used to establish whether the extents of observed clusters of significant connected edges were due to chance. Two clusters in the long delay group survived correction: a 15-edge cluster of positive correlations ($p = .016$) and a 15-edge cluster of negative correlations ($p = .018$). The cluster of connected positive correlations included edges between the hippocampus, the DMN (NW 15, 16), the Parietal Memory Network (NW 11), the Frontoparietal Network (NW 12, 13), and Limbic Networks (NW 9, 10). The cluster of connected negative correlations included sensory networks (NW 1, 2, 3, 4, 14), the Dorsal Attention Network (NW 5, 6), and parts of the Ventral Attention Network (NW 7). Included in these two large-scale network systems were also edges connecting the two clusters: connectivity between Parietal Memory NW 11 and sensory NW 2, as well as between DMN NW 16 and sensory NW 2 showed a positive relationship with source memory performance. Connectivity between DMN NW 17 and Dorsal/Ventral Attention NW 6/7, on the other hand, showed a negative relationship with memory.

Connectivity levels within the significant positive cluster and the significant negative cluster were strongly negatively correlated across participants in the long delay group (*rho* = -.83, $p < .0001$; Figure 4). Based on the observation that some participants showed higher connectivity levels within the positive cluster compared to the negative cluster, and vice versa, we ran a follow-up analysis splitting the long delay sample into those who showed stronger connectivity levels within the positive cluster compared to the negative (N=18) and those who showed stronger connectivity levels within the negative cluster compared to the positive (N=19). An independent sample t-test confirmed that participants with higher coupling in the positive cluster at rest retained significantly more source information over a retention interval of weeks compared to those who showed higher coupling in the negative cluster ($t(35)=3.94$; $p < .0005$).

--- INSERT FIGURE 4 ABOUT HERE ---

Finally, a direct test of the difference between the observed correlations in the two groups confirmed that the relationships between network connectivity and source memory performance were unique to the long delay group (Figure 3C). Furthermore, after extracting mean *rho* from the two significant clusters, a comparison of correlation coefficients in the two groups showed that the observed relationship was significantly stronger in the long delay group in both the positive (one-tailed $p = .019$) and in the negative (one-tailed $p = .015$) cluster. For descriptive purposes, Figure 3D shows plots of average connectivity levels within significant clusters against source memory performance in the two groups.

No significant clusters of correlations between network connectivity and memory performance were observed in the short delay group. The main findings, source memory performance in the long delay group correlating positively with connectivity within a DMN-centered network system and negatively with connectivity within a task-positive network system, remained robust in several control analyses: 1) Controlling for candidate confounds (delay interval in the long delay group, IQ, and working memory capacity; Supplementary Figure 3), 2) Using different cluster-forming thresholds (Supplementary Figure 4) 3) Using uncorrected source memory scores as memory performance measure (Supplementary Figure 5), 4) Separating the bilateral 17-network parcellation into unilateral networks (Supplementary Figure 6). Note however that all networks discovered by Yeo and colleagues in their optimal parcellation were bilateral (Yeo et al., 2011). Finally, the negative correlation between connectivity levels in the two significant clusters was also found in the short delay group, indicating that the observed antagonistic relationship is stable across samples (Supplementary Figure 7).

3.3. Antagonistic interactions between cortical networks

The observed significant negative relationship between memory performance weeks after encoding and pre-encoding connectivity within a sensory-dominated network constellation suggests that sensory decoupling benefits long-term memory performance. Moreover, the opposite (positive) relationship between memory performance and connectivity within a Parietal Memory/DMN-centered system suggests that the two systems, "Sensory" and "DMN", may interact in an antagonistic fashion. Pursuing this hypothesis, we combined rsFC estimates from all 87 participants to characterize connectivity patterns between the investigated networks (i.e., independent of behavior).

--- INSERT FIGURE 5 ABOUT HERE ---

We operationalized sensory coupling as the average connectivity within unique edges in the upper left 5x5 quadrant of the connectivity matrix; i.e. connectivity within and between visual (Yeo NW 1+2), somatomotor (Yeo NW 3+4), and auditory (Yeo NW 14) networks. We first investigated whether individual differences in connectivity between the two significant "Sensory" and "DMN" clusters shown in Figure 3B predicted degree of sensory coupling. Here, we pursued the edges found to be significantly and uniquely associated with memory performance in the long delay group and connecting the two systems (i.e., falling within the upper right quadrant of the matrix in Figure 3C). The networks included in the analysis are shown in Figure 5A. Figure 5B shows that connectivity levels between Parietal Memory NW 11 / DMN NW 16 and visual sensory NW 2 correlated negatively with connectivity within the sensory networks (*rho* = -.25; Holm-Bonferroni adjusted p = .018). The same two connecting edges were *positively* correlated with connectivity within DMN/Parietal Memory network (*rho* = .29; adjusted p = .013). In other words, participants with a strong connection of the two systems via NW 11/NW 16 and NW 2 tended to show low levels of sensory coupling and high levels

of connectivity within a DMN-centered system. Similarly, connectivity levels between DMN NW 17 and Dorsal Attention NW 6 correlated positively with connectivity within sensory networks (*rho* = .43; adjusted *p* =.0001), and *negatively* with connectivity within the DMN and Parietal Memory network (*rho* = -.37; adjusted *p* = .0013; Figure 5C; Supplementary Figure 8). Thus, connectivity levels within memory-relevant edges that connect the "DMN" and "Sensory" systems was linked with sensory coupling and DMN synchronicity in a manner consistent with the observed relationships between connectivity and memory performance.

Finally, we explicitly tested the prediction that a high level of connectivity within the "DMN" system is associated with sensory decoupling, that is: the two systems exist in an antagonistic relationship. While we above confirmed that the two significant clusters of connectivity-memory relationships found in the long-delay group were negatively correlated, we here extracted mean connectivity estimates from edges in the "DMN" system significantly and uniquely associated with memory performance (i.e. falling within the lower right quadrant of the matrix in Figure 3C). This included interactions within and between Parietal Memory NW 11 and DMN NW 15 and 16. We observed a strong negative correlation between individual differences in connectivity within this "DMN" cluster and connectivity within the sensory networks (*rho* = -.61; $p < .0001$; Supplementary Figure 7), demonstrating that individuals with strong resting state connectivity within DMN and Parietal Memory Network regions show lower sensory coupling.

4. Discussion

The present results show that participants characterized by strong decoupling between DMN and perceptual regions are more efficient at establishing durable long-term memories. We observed a positive correlation between amount of episodic memories retained weeks after encoding and individual differences in the ability to engage a large-scale network system involving the DMN, as well as the hippocampus, frontoparietal, and limbic networks. The opposite relationship was found with perceptual regions and external attention networks, in which low levels of synchronicity were beneficial for long-term recollection. Complementing these results, we found that a DMN-centered network constellation was anticorrelated with sensory networks, and that the degree of anticorrelation was reflected in the strength of interacting links between the two systems. The present findings thus indicate that the regulation of networks with possible opposing effects on cognition is important in facilitating stabilization of episodic memories over extended time intervals.

4.1 DMN-recruitment and perceptual decoupling predict long-term memory

The significant cluster of positive correlations between long-term memory performance and connectivity contained edges linking subnetworks of the DMN and hippocampus to Limbic networks, the Frontoparietal network and the recently proposed Parietal Memory network (Gilmore et al., 2015). Together with the Parietal Memory network, communication within DMN at rest seems to be of particular importance for ongoing processes related to establishing durable long-term memories, as DMN connectivity was uniquely associated with performance in the long delay group (cf. Figure 3C). A massive amount of research has gone into describing the DMNs role in cognition (Andrews-Hanna et al., 2014), and several lines of evidence point to it being central in the forming and accessing of memory representations. Degeneration of DMN structures and changes in rsFC within the DMN is seen with increased age and in particular in amnestic

conditions such as Alzheimer's disease (Jones et al., 2011; Mevel et al., 2011; Sala-Llonch et al., 2015), and has been linked to reduced memory performance in healthy controls (Fjell et al., 2015; Mevel et al., 2013; Persson et al., 2014). Moreover, DMN structures have consistently been found to be differentially recruited during episodic memory encoding and retrieval (Huijbers et al., 2012; Vannini et al., 2013), and more strongly activated during retrieval of remote than recently encoded memories (Gais et al., 2007; Takashima et al., 2007). Also, the DMN is associated with autobiographical retrieval and updating (Philippi et al., 2014; Schacter et al., 2012). One explanation for the apparent important role of DMN in memory function comes from a series of recent experimental investigations finding that DMN is a system generally involved in cognitive operations on representations not available to the senses (Konishi et al., 2015; Smallwood et al., 2013; Spreng et al., 2014). In a global workspace framework, high DMN engagement is thus an indication that task-unrelated/stimulus-independent thoughts are dominating awareness at a given moment, i.e. attention is oriented internally (Smallwood et al., 2012). Importantly, recent investigations have demonstrated that neuronal activity in perceptual brain regions and, correspondingly, processing of external input, is attenuated during periods of task-unrelated thoughts, a phenomenon termed perceptual decoupling (Baird et al., 2014; Braboszcz and Delorme, 2011; Kam et al., 2011; Schooler et al., 2011; Smallwood et al., 2013).

Our data supports the notion that DMN-engagement and perceptual decoupling constitute opposing processes, as the DMN and perceptual networks were shown to be strongly anticorrelated at rest. Furthermore, while high levels of connectivity within DMN-networks correlated positively with long-term memory performance, the opposite relationship was found within sensory networks. Recent studies support the view that consolidation results from re-activation of labile internal memory representations during off-task periods (Deuker et al., 2013; Gregory et al., 2014; Gruber et al., 2016; Schlichting and Preston, 2014; Staresina et al., 2013). However, while these studies have

demonstrated spontaneous re-occurrence of encoding stimuli during post-learning rest, it remains an open question for future research whether such re-surfacing of internal representations occur with higher frequency in individuals with strong DMN connectivity during task-independent rest.

Interestingly, the cluster of positive correlations between long-term memory performance and connectivity also contained edges between the frontoparietal network and DMN. The frontoparietal network is commonly considered to be part of the external attention system (EAS) and anti-correlated with DMN during rest (Anticevic et al., 2012). However, recent studies have found evidence for functional integration of these network systems during certain cognitive tasks, including mind-wandering (Christoff et al., 2009), memory recollection (Fornito et al., 2012) and memory search (Kragel and Polyn, 2013). Similarly, the Parietal Memory network has been associated with core memory functions such as distinguishing between novel and familiar items (Gilmore et al., 2015). In sum, the rsFC interactions observed to be relevant for long-term memory in the present study occur between regions and networks with documented roles in central memory operations.

4.2. The Dorsal Attention Network as a regulating intermediate between DMN and sensory networks

The cluster of negative correlations between long-term memory performance and connectivity contained edges linking sensory networks to the Dorsal Attention Network (DAN; NW 5 and 6) and parts of the Ventral Attention Network (NW 7). A closer look at the connectivity-behavior correlations within and between the attention networks (i.e., in Figure 3A) shows that no strong trends existed between the degree of communication among these networks and memory performance. Rather, their memory-relevant communication was found in their connectivity with sensory networks which, when low, was associated with better long-term memory performance. An indication of how

this attentional-sensory decoupling may be regulated comes from the observation that strength of connectivity within sensory regions was reflected in the connectivity between DMN regions (NW 17) and the Dorsal Attention Network (NW 6; Figure 5A). As shown in Figure 5C, strong levels of connectivity within the DMN was associated with weak coupling between DMN and the Dorsal Attention Network (DAN). Weak DMN-DAN coupling was further associated with low connectivity levels between DAN and sensory networks, and this desynchronization was associated with sensory decoupling (Supplementary Figure 8). Thus, a complex interplay between DMN and DAN may underlie sensory decoupling, and, as suggested by similar observations in the literature, internally guided cognition (Kragel and Polyn, 2013; Shapira-Lichter et al., 2013; Smallwood et al., 2012; Vincent et al., 2008).

Although previous studies using individual differences in rsFC to index trait-level episodic memory capacity after short delay intervals have found local relationships within the hippocampal complex (Wang et al., 2010; Wig et al., 2008), we did not find any robust links between cortical network connectivity and source memory performance in the short delay group. These previous studies focused specifically on the medial temporal lobes and utilized free recall as memory capacity measure, either alone (Wang et al., 2010), or combined with verbal recognition capacity into a PCA score (Wig et al., 2008). The current study focused on interactions between large-scale networks and used a stringent measure of source memory capacity as behavioral measure, and these methodological differences may explain the apparent inconsistencies with earlier reports.

Interestingly, a recent study found that individual differences in autobiographical recall in an adult lifespan sample correlated with rsFC between parts of the DMN and hippocampus (Mevel et al., 2013). Autobiographical recall relates to memory for events that occurred far back in time, and can to some extent be argued to resemble the long

delay condition in our experiment. In the same study, no correspondence was found between DMN connectivity and performance on tests of episodic memory capacity utilizing brief retention delays. Obviously, mechanisms supporting successful retention over minutes and hours are relevant for systems consolidation, as memory for an event after a short delay is a prerequisite for that event to be remembered after delays of days and weeks (Carr et al., 2010; Liu et al., 2013). However, in our sample of young healthy adults, large-scale neocortical network connectivity patterns seem to reflect processes relevant for long-term memory stabilization only. We have recently demonstrated that encoding of durable episodic memories is associated with hippocampal-neocortical connectivity signatures not critical for the encoding of more short-lived memories (Sneve et al., 2015), and the present results complement the notion that systems consolidation of enduring memory traces is partly dependent on processes less important for immediate recollection.

4.3. Limitations

A limitation of the current study is the dependence of one single rsfMRI scan to estimate individual brain connectivity patterns. Recent research has shown that, while there are reliable components to be found in rsFC measures, they are also influenced by transient, state-dependent components (e.g., Geerligs et al., 2015; Hutchison et al., 2013). Although the implications such findings have on the interpretation of individual differences in rsFC are currently being debated (e.g., Laumann et al., 2016), it is likely that factors such as fluctuations between alertness and drowsiness introduce some instability in the rsFC measure (Chang et al., 2016).

Finally, we observed strong positive correlations between edges involving the two Limbic networks (NW 9 and 10) and memory performance in the long delay group. These regions are known to suffer from susceptibility artifacts due to their proximity to air-tissue boundaries. Even after B0-correction of participants' fMRI data, we observed

low average connectivity levels in all edges involving the two networks (e.g., see Figure 3B). The findings involving these networks thus have to be to be interpreted with caution.

4.4. Conclusion

In sum, we here show that individual differences in rsFC connectivity within and between large-scale cortical networks and the hippocampus explain, in part, behavioral variability attributable to ongoing systems consolidation processes. The selective relationship between observed connectivity patterns and true long-term memory capacity, operationalized as successful retention after weeks rather than minutes, suggests that these differences in network interactions are important for slow or repeated cognitive processes that are extended in time.

Acknowledgements

This work was supported by the European Research Council's Starting Grant scheme (to K.B.W project number 313440 and A.M.F. project number 283634), the Norwegian Research Council (to A.M.Fjell and K.B.Walhovd), and the Department of Psychology, University of Oslo). We would like to thank Professor Lars Nyberg for helpful comments on earlier drafts of the manuscript and Didac Vidal Piñeiro for help with the analyses.

References

Andrews-Hanna, J.R., Smallwood, J., Spreng, R.N., 2014. The default network and self-generated thought: component processes, dynamic control, and clinical relevance. Ann. N. Y. Acad. Sci. 1316, 29–52. doi:10.1111/nyas.12360

Anticevic, A., Cole, M.W., Murray, J.D., Corlett, P.R., Wang, X.-J., Krystal, J.H., 2012. The role of default network deactivation in cognition and disease. Trends Cogn. Sci. 16, 584–92. doi:10.1016/j.tics.2012.10.008

Baird, B., Smallwood, J., Lutz, A., Schooler, J.W., 2014. The Decoupled Mind: Mind-wandering Disrupts Cortical Phase-locking to Perceptual Events. J. Cogn. Neurosci. 26, 2596–2607. doi:10.1162/jocn_a_00656

Beck, A.T., Steer, R.A., 1987. Beck Depression Inventory Scoring Manual. The Psychological Corporation, New York.

Ben-Yakov, A., Dudai, Y., 2011. Constructing Realistic Engrams: Poststimulus Activity of Hippocampus and Dorsal Striatum Predicts Subsequent Episodic Memory. J. Neurosci. 31, 9032–9042. doi:10.1523/JNEUROSCI.0702-11.2011

Ben-Yakov, A., Eshel, N., Dudai, Y., 2013. Hippocampal immediate poststimulus activity in the encoding of consecutive naturalistic episodes. J. Exp. Psychol. Gen. 142, 1255–1263. doi:10.1037/a0033558

Ben-Yakov, A., Rubinson, M., Dudai, Y., 2014. Shifting Gears in Hippocampus: Temporal Dissociation between Familiarity and Novelty Signatures in a Single Event. J. Neurosci. 34, 12973–12981. doi:10.1523/JNEUROSCI.1892-14.2014

Braboszcz, C., Delorme, A., 2011. Lost in thoughts: Neural markers of low alertness during mind wandering. Neuroimage 54, 3040–3047. doi:10.1016/j.neuroimage.2010.10.008

Buckner, R.L., Andrews-Hanna, J.R., Schacter, D.L., 2008. The brain's default network: anatomy, function, and relevance to disease. Ann. N. Y. Acad. Sci. 1124, 1–38. doi:10.1196/annals.1440.011

Carr, V.A., Viskontas, I. V., Engel, S.A., Knowlton, B.J., 2010. Neural activity in the hippocampus and perirhinal cortex during encoding is associated with the durability of episodic memory. J. Cogn. Neurosci. 22, 2652–62. doi:10.1162/jocn.2009.21381

Chang, C., Leopold, D.A., Schölvinck, M.L., Mandelkow, H., Picchioni, D., Liu, X., Ye, F.Q., Turchi, J.N., Duyn, J.H., 2016. Tracking brain arousal fluctuations with fMRI. Proc. Natl. Acad. Sci. U. S. A. 113, 4518–23. doi:10.1073/pnas.1520613113

Christoff, K., Gordon, A.M., Smallwood, J., Smith, R., Schooler, J.W., 2009. Experience sampling during fMRI reveals default network and executive system contributions to mind wandering. Proc. Natl. Acad. Sci. U. S. A. 106, 8719–24. doi:10.1073/pnas.0900234106

Daselaar, S.M., Prince, S.E., Dennis, N. a, Hayes, S.M., Kim, H., Cabeza, R., 2009. Posterior midline and ventral parietal activity is associated with retrieval success and encoding failure. Front. Hum. Neurosci. 3, 13. doi:10.3389/neuro.09.013.2009

Desikan, R.S., Ségonne, F., Fischl, B., Quinn, B.T., Dickerson, B.C., Blacker, D., Buckner, R.L., Dale, A.M., Maguire, R.P., Hyman, B.T., Albert, M.S., Killiany, R.J., 2006. An automated labeling system for subdividing the human cerebral cortex on MRI scans into gyral based regions of interest. Neuroimage 31, 968–980. doi:DOI: 10.1016/j.neuroimage.2006.01.021

Deuker, L., Olligs, J., Fell, J., Kranz, T.A., Mormann, F., Montag, C., Reuter, M., Elger, C.E., Axmacher, N., 2013. Memory Consolidation by Replay of Stimulus-Specific Neural Activity. J. Neurosci. 33, 19373–19383. doi:10.1523/JNEUROSCI.0414-13.2013

Diekelmann, S., Born, J., 2010. The memory function of sleep. Nat. Rev. Neurosci. 11, 114–26. doi:10.1038/nrn2762

Dosenbach, N.U.F., Fair, D. a, Miezin, F.M., Cohen, A.L., Wenger, K.K., Dosenbach, R. a T., Fox, M.D., Snyder, A.Z., Vincent, J.L., Raichle, M.E., Schlaggar, B.L., Petersen, S.E., 2007. Distinct brain networks for adaptive and stable task control in humans. Proc. Natl. Acad. Sci. U. S. A. 104, 11073–8. doi:10.1073/pnas.0704320104

Dudai, Y., Karni, A., Born, J., 2015. The Consolidation and Transformation of Memory. Neuron 88, 20–32. doi:10.1016/j.neuron.2015.09.004

Eichele, T., Debener, S., Calhoun, V.D., Specht, K., Engel, A.K., Hugdahl, K., von Cramon, D.Y., Ullsperger, M., 2008. Prediction of human errors by maladaptive changes in event-related brain networks. Proc. Natl. Acad. Sci. U. S. A. 105, 6173–8. doi:10.1073/pnas.0708965105

Fischl, B., Salat, D.H., Busa, E., Albert, M., Dieterich, M., Haselgrove, C., van der Kouwe, A., Killiany, R., Kennedy, D., Klaveness, S., Montillo, A., Makris, N., Rosen, B., Dale, A.M., 2002. Whole brain segmentation: automated labeling of neuroanatomical structures in the human brain. Neuron 33, 341–355.

Fischl, B., Salat, D.H., van der Kouwe, A.J.W., Makris, N., Ségonne, F., Quinn, B.T., Dale, A.M., 2004a. Sequence-independent segmentation of magnetic resonance images. Neuroimage 23, S69–S84. doi:DOI: 10.1016/j.neuroimage.2004.07.016

Fischl, B., Sereno, M.I., Dale, A.M., 1999a. Cortical Surface-Based Analysis: II: Inflation, Flattening, and a Surface-Based Coordinate System. Neuroimage 9, 195–207.

Fischl, B., Sereno, M.I., Tootell, R.B.H., Dale, A.M., 1999b. High-resolution intersubject averaging and a coordinate system for the cortical surface. Hum. Brain Mapp. 8, 272–284. doi:10.1002/(SICI)1097-0193(1999)8:4<272::AID-HBM10>3.0.CO;2-4

Fischl, B., van der Kouwe, A., Destrieux, C., Halgren, E., Ségonne, F., Salat, D.H., Busa, E.,

Seidman, L.J., Goldstein, J., Kennedy, D., Caviness, V., Makris, N., Rosen, B., Dale, A.M., 2004b. Automatically Parcellating the Human Cerebral Cortex. Cereb. Cortex 14, 11–22. doi:10.1093/cercor/bhg087

Fjell, A.M., Sneve, M.H., Grydeland, H., Storsve, A.B., de Lange, A.M.G., Amlien, I.K., Røgeberg, O.J., Walhovd, K.B., 2015. Functional connectivity change across multiple cortical networks relates to episodic memory changes in aging. Neurobiol. Aging 36, 3255–3268. doi:10.1016/j.neurobiolaging.2015.08.020

Folstein, M.F., Folstein, S.E., McHugh, P.R., 1975. "Mini-mental state". A practical method for grading the cognitive state of patients for the clinician. J. Psychiatr. Res. 12, 189–198. doi:0022-3956(75)90026-6 [pii]

Fornito, A., Harrison, B.J., Zalesky, A., Simons, J.S., 2012. Competitive and cooperative dynamics of large-scale brain functional networks supporting recollection. Proc. Natl. Acad. Sci. U. S. A. 109, 12788–93. doi:10.1073/pnas.1204185109

Fox, M.D., Snyder, A.Z., Vincent, J.L., Corbetta, M., Van Essen, D.C., Raichle, M.E., 2005. The human brain is intrinsically organized into dynamic, anticorrelated functional networks. Proc. Natl. Acad. Sci. U. S. A. 102, 9673–8. doi:10.1073/pnas.0504136102

Frankland, P.W., Bontempi, B., 2005. The organization of recent and remote memories. Nat. Rev. Neurosci. 6, 119–30. doi:10.1038/nrn1607

Gais, S., Albouy, G., Boly, M., Dang-Vu, T.T., Darsaud, A., Desseilles, M., Rauchs, G., Schabus, M., Sterpenich, V., Vandewalle, G., Maquet, P., Peigneux, P., 2007. Sleep transforms the cerebral trace of declarative memories. Proc. Natl. Acad. Sci. U. S. A. 104, 18778–83. doi:10.1073/pnas.0705454104

Geerligs, L., Rubinov, M., Cam-CAN, Henson, R.N., 2015. State and Trait Components of Functional Connectivity: Individual Differences Vary with Mental State. J. Neurosci. 35, 13949–13961. doi:10.1523/JNEUROSCI.1324-15.2015

Gilmore, A.W., Nelson, S.M., McDermott, K.B., 2015. A parietal memory network revealed by multiple MRI methods. Trends Cogn. Sci. 19, 534–43. doi:10.1016/j.tics.2015.07.004

Gregory, M.D., Agam, Y., Selvadurai, C., Nagy, A., Vangel, M., Tucker, M., Robertson, E.M., Stickgold, R., Manoach, D.S., 2014. Resting state connectivity immediately following learning correlates with subsequent sleep-dependent enhancement of motor task performance. Neuroimage 102 Pt 2, 666–73. doi:10.1016/j.neuroimage.2014.08.044

Gruber, M.J., Ritchey, M., Wang, S., Doss, M.K., Ranganath, C., 2016. Post-learning Hippocampal Dynamics Promote Preferential Retention of Rewarding Events. Neuron 89, 1110–1120. doi:10.1016/j.neuron.2016.01.017

Hallquist, M.N., Hwang, K., Luna, B., 2013. The Nuisance of Nuisance Regression: Spectral Misspecification in a Common Approach to Resting-State fMRI Preprocessing Reintroduces Noise and Obscures Functional Connectivity. Neuroimage 82C, 208–225. doi:10.1016/j.neuroimage.2013.05.116

Han, C.E., Yoo, S.W., Seo, S.W., Na, D.L., Seong, J.-K., 2013. Cluster-based statistics for brain connectivity in correlation with behavioral measures. PLoS One 8, e72332. doi:10.1371/journal.pone.0072332

Huijbers, W., Vannini, P., Sperling, R.A., C M, P., Cabeza, R., Daselaar, S.M., 2012. Explaining the encoding/retrieval flip: memory-related deactivations and activations in the posteromedial cortex. Neuropsychologia 50, 3764–74. doi:10.1016/j.neuropsychologia.2012.08.021

Hutchison, R.M., Womelsdorf, T., Allen, E.A., Bandettini, P.A., Calhoun, V.D., Corbetta, M., Della Penna, S., Duyn, J.H., Glover, G.H., Gonzalez-Castillo, J., Handwerker, D.A., Keilholz, S., Kiviniemi, V., Leopold, D.A., de Pasquale, F., Sporns, O., Walter, M.,

Chang, C., 2013. Dynamic functional connectivity: Promise, issues, and interpretations. Neuroimage 80, 360–378. doi:10.1016/j.neuroimage.2013.05.079

Jones, D.T., MacHulda, M.M., Vemuri, P., McDade, E.M., Zeng, G., Senjem, M.L., Gunter, J.L., Przybelski, S.A., Avula, R.T., Knopman, D.S., Boeve, B.F., Petersen, R.C., Jack, C.R., 2011. Age-related changes in the default mode network are more advanced in Alzheimer disease. Neurology 77, 1524–1531. doi:10.1212/WNL.0b013e318233b33d

Kam, J.W.Y., Dao, E., Farley, J., Fitzpatrick, K., Smallwood, J., Schooler, J.W., Handy, T.C., 2011. Slow fluctuations in attentional control of sensory cortex. J. Cogn. Neurosci. 23, 460–70. doi:10.1162/jocn.2010.21443

Kelly, a M.C., Uddin, L.Q., Biswal, B.B., Castellanos, F.X., Milham, M.P., 2008. Competition between functional brain networks mediates behavioral variability. Neuroimage 39, 527–37. doi:10.1016/j.neuroimage.2007.08.008

Kim, H., 2011. Neural activity that predicts subsequent memory and forgetting: a meta-analysis of 74 fMRI studies. Neuroimage 54, 2446–61. doi:10.1016/j.neuroimage.2010.09.045

Konishi, M., McLaren, D.G., Engen, H., Smallwood, J., 2015. Shaped by the Past: The Default Mode Network Supports Cognition that Is Independent of Immediate Perceptual Input. PLoS One 10, e0132209. doi:10.1371/journal.pone.0132209

Kragel, J.E., Polyn, S.M., 2013. Functional Interactions Between Large-Scale Networks During Memory Search. Cereb. Cortex 1–13. doi:10.1093/cercor/bht258

Laumann, T.O., Snyder, A.Z., Mitra, A., Gordon, E.M., Gratton, C., Adeyemo, B., Gilmore, A.W., Nelson, S.M., Berg, J.J., Greene, D.J., McCarthy, J.E., Tagliazucchi, E., Laufs, H., Schlaggar, B.L., Dosenbach, N.U.F., Petersen, S.E., 2016. On the Stability of BOLD fMRI Correlations. Cereb. Cortex 1–14. doi:10.1093/cercor/bhw265

Liu, Q., Dong, Q., Chen, C., Xue, G., 2013. Neural processes during encoding support durable memory. Neuroimage 88C, 1–9. doi:10.1016/j.neuroimage.2013.11.031

Mevel, K., Chetelat, G., Eustache, F., Desgranges, B., 2011. The default mode network in healthy aging and Alzheimer's disease. Int J Alzheimers Dis 2011, 535816. doi:10.4061/2011/535816

Mevel, K., Landeau, B., Fouquet, M., La Joie, R., Villain, N., Mézenge, F., Perrotin, A., Eustache, F., Desgranges, B., Chételat, G., 2013. Age effect on the default mode network, inner thoughts, and cognitive abilities. Neurobiol. Aging 34, 1292–301. doi:10.1016/j.neurobiolaging.2012.08.018

Myers, L., Sirois, M.J., 2006. Spearman Correlation Coefficients, Differences between, in: Encyclopedia of Statistical Sciences. John Wiley & Sons, Inc., Hoboken, NJ, USA, pp. 1–2. doi:10.1002/0471667196.ess5050.pub2

Nadel, L., Moscovitch, M., 1997. Memory consolidation, retrograde amnesia and the hippocampal complex. Curr. Opin. Neurobiol. 7, 217–27.

Nichols, T.E., Holmes, A.P., 2002. Nonparametric permutation tests for functional neuroimaging: a primer with examples. Hum. Brain Mapp. 15, 1–25.

Persson, J., Pudas, S., Nilsson, L.-G., Nyberg, L., 2014. Longitudinal assessment of default-mode brain function in aging. Neurobiol. Aging 35, 2107–17. doi:10.1016/j.neurobiolaging.2014.03.012

Philippi, C.L., Tranel, D., Duff, M., Rudrauf, D., 2014. Damage to the default mode network disrupts autobiographical memory retrieval. Soc. Cogn. Affect. Neurosci. 318–326. doi:10.1093/scan/nsu070

Pruim, R.H.R., Mennes, M., Buitelaar, J.K., Beckmann, C.F., 2015. Evaluation of ICA-AROMA and alternative strategies for motion artifact removal in resting-state fMRI. Neuroimage 112, 278–287. doi:10.1016/j.neuroimage.2015.02.063

Raichle, M.E., MacLeod, A.M., Snyder, A.Z., Powers, W.J., Gusnard, D.A., Shulman, G.L., 2001. A default mode of brain function. Proc. Natl. Acad. Sci. U. S. A. 98, 676–82. doi:10.1073/pnas.98.2.676

Ranganath, C., Ritchey, M., 2012. Two cortical systems for memory-guided behaviour. Nat. Rev. Neurosci. 13, 713–26. doi:10.1038/nrn3338

Rauschecker, J.P., Scott, S.K., 2009. Maps and streams in the auditory cortex: nonhuman primates illuminate human speech processing. Nat. Neurosci. 12, 718–24. doi:10.1038/nn.2331

Sadaghiani, S., Poline, J.-B., Kleinschmidt, A., D'Esposito, M., 2015. Ongoing dynamics in large-scale functional connectivity predict perception. Proc. Natl. Acad. Sci. 112, 201420687. doi:10.1073/pnas.1420687112

Sala-Llonch, R., Bartrés-Faz, D., Junqué, C., 2015. Reorganization of brain networks in aging: a review of functional connectivity studies. Front. Psychol. 6, 663. doi:10.3389/fpsyg.2015.00663

Salimi-Khorshidi, G., Douaud, G., Beckmann, C.F., Glasser, M.F., Griffanti, L., Smith, S.M., 2014. Automatic denoising of functional MRI data: Combining independent component analysis and hierarchical fusion of classifiers. Neuroimage 90, 449–468. doi:10.1016/j.neuroimage.2013.11.046

Schacter, D.L., Addis, D.R., Hassabis, D., Martin, V.C., Spreng, R.N., Szpunar, K.K., 2012. The Future of Memory: Remembering, Imagining, and the Brain. Neuron 76, 677–694. doi:10.1016/j.neuron.2012.11.001

Schlichting, M.L., Preston, A.R., 2014. Memory reactivation during rest supports upcoming learning of related content. Proc. Natl. Acad. Sci. U. S. A. 111, 15845–50. doi:10.1073/pnas.1404396111

Schooler, J.W., Smallwood, J., Christoff, K., Handy, T.C., Reichle, E.D., Sayette, M.A., 2011.

Meta-awareness, perceptual decoupling and the wandering mind. Trends Cogn. Sci. 15, 319–326. doi:10.1016/j.tics.2011.05.006

Seeley, W.W., Menon, V., Schatzberg, A.F., Keller, J., Glover, G.H., Kenna, H., Reiss, A.L., Greicius, M.D., 2007. Dissociable intrinsic connectivity networks for salience processing and executive control. J. Neurosci. 27, 2349–56. doi:10.1523/JNEUROSCI.5587-06.2007

Shapira-Lichter, I., Oren, N., Jacob, Y., Gruberger, M., Hendler, T., 2013. Portraying the unique contribution of the default mode network to internally driven mnemonic processes. Proc. Natl. Acad. Sci. U. S. A. 110, 4950–5. doi:10.1073/pnas.1209888110

Silver, N., Dunlap, W., 1987. Averaging correlation coefficients: Should Fisher's z transformation be used? J. Appl. Psychol. 72, 1979–1981.

Smallwood, J., Brown, K., Baird, B., Schooler, J.W., 2012. Cooperation between the default mode network and the frontal-parietal network in the production of an internal train of thought. Brain Res. 1428, 60–70. doi:10.1016/j.brainres.2011.03.072

Smallwood, J., Tipper, C., Brown, K., Baird, B., Engen, H., Michaels, J.R., Grafton, S., Schooler, J.W., 2013. Escaping the here and now: Evidence for a role of the default mode network in perceptually decoupled thought. Neuroimage 69, 120–125. doi:10.1016/j.neuroimage.2012.12.012

Sneve, M.H., Grydeland, H., Nyberg, L., Bowles, B., Amlien, I.K., Langnes, E., Walhovd, K.B., Fjell, A.M., 2015. Mechanisms Underlying Encoding of Short-Lived Versus Durable Episodic Memories. J. Neurosci. 35, 5202–5212. doi:10.1523/JNEUROSCI.4434-14.2015

Spreng, R.N., Dupre, E., Selarka, D., Garcia, J., Gojkovic, S., Mildner, J., Luh, X.W., Turner, G.R., 2014. Goal-Congruent Default Network Activity Facilitates Cognitive Control. J.

Neurosci. 34, 14108–14114. doi:10.1523/JNEUROSCI.2815-14.2014

Squire, L.R., Alvarez, P., 1995. Retrograde amnesia and memory consolidation: a neurobiological perspective. Curr. Opin. Neurobiol. 5, 169–77.

Stanislaw, H., Todorov, N., 1999. Calculation of signal detection theory measures. Behav. Res. Methods. Instrum. Comput. 31, 137–49.

Staresina, B.P., Alink, A., Kriegeskorte, N., Henson, R.N., 2013. Awake reactivation predicts memory in humans. Proc. Natl. Acad. Sci. U. S. A. 110, 21159–64. doi:10.1073/pnas.1311989110

Stevens, W.D., Buckner, R.L., Schacter, D.L., 2010. Correlated low-frequency BOLD fluctuations in the resting human brain are modulated by recent experience in category-preferential visual regions. Cereb. Cortex 20, 1997–2006. doi:10.1093/cercor/bhp270

Stickgold, R., 2013. Parsing the role of sleep in memory processing. Curr. Opin. Neurobiol. 23, 847–53. doi:10.1016/j.conb.2013.04.002

Takashima, a, Nieuwenhuis, I.L., Rijpkema, M., Petersson, K.M., Jensen, O., Fernandez, G., 2007. Memory trace stabilization leads to large-scale changes in the retrieval network: a functional MRI study on associative memory. Learn Mem 14, 472–479. doi:10.1101/lm.605607

Tambini, A., Davachi, L., 2013. Persistence of hippocampal multivoxel patterns into postencoding rest is related to memory. Proc. Natl. Acad. Sci. U. S. A. 110, 19591–6. doi:10.1073/pnas.1308499110

Tambini, A., Ketz, N., Davachi, L., 2010. Enhanced Brain Correlations during Rest Are Related to Memory for Recent Experiences. Neuron 65, 280–290. doi:10.1016/j.neuron.2010.01.001

Van Dijk, K.R.A., Hedden, T., Venkataraman, A., Evans, K.C., Lazar, S.W., Buckner, R.L.,

2010. Intrinsic functional connectivity as a tool for human connectomics: theory, properties, and optimization. J. Neurophysiol. 103, 297–321. doi:10.1152/jn.00783.2009

van Kesteren, M.T.R., Fernández, G., Norris, D.G., Hermans, E.J., 2010. Persistent schema-dependent hippocampal-neocortical connectivity during memory encoding and postencoding rest in humans. Proc. Natl. Acad. Sci. U. S. A. 107, 7550–5. doi:10.1073/pnas.0914892107

Vannini, P., Hedden, T., Huijbers, W., Ward, A., Johnson, K.A., Sperling, R.A., 2013. The Ups and Downs of the Posteromedial Cortex: Age- and Amyloid-Related Functional Alterations of the Encoding/Retrieval Flip in Cognitively Normal Older Adults. Cereb. Cortex 23, 1317–1328. doi:10.1093/cercor/bhs108

Vincent, J.L., Kahn, I., Snyder, A.Z., Raichle, M.E., Buckner, R.L., 2008. Evidence for a frontoparietal control system revealed by intrinsic functional connectivity. J. Neurophysiol. 100, 3328–42. doi:10.1152/jn.90355.2008

Wang, L., Negreira, A., LaViolette, P., Bakkour, A., Sperling, R.A., Dickerson, B.C., 2010. Intrinsic interhemispheric hippocampal functional connectivity predicts individual differences in memory performance ability. Hippocampus 20, 345–51. doi:10.1002/hipo.20771

Wechsler, D., 1999. Wechsler abbreviated scale of intelligence. The Psychological Corporation, San Antonio, Texas.

Wig, G.S., Grafton, S.T., Demos, K.E., Wolford, G.L., Petersen, S.E., Kelley, W.M., 2008. Medial temporal lobe BOLD activity at rest predicts individual differences in memory ability in healthy young adults. Proc. Natl. Acad. Sci. U. S. A. 105, 18555–60. doi:10.1073/pnas.0804546105

Wiltgen, B.J., Brown, R.A.M., Talton, L.E., Silva, A.J., 2004. New circuits for old memories:

The role of the neocortex in consolidation. Neuron 44, 101–108. doi:10.1016/j.neuron.2004.09.015

Yan, C.G., Craddock, R.C., Zuo, X.N., Zang, Y.F., Milham, M.P., 2013. Standardizing the intrinsic brain: Towards robust measurement of inter-individual variation in 1000 functional connectomes. Neuroimage 80, 246–262. doi:10.1016/j.neuroimage.2013.04.081

Yeo, B.T.T., Krienen, F.M., Sepulcre, J., Sabuncu, M.R., Lashkari, D., Hollinshead, M., Roffman, J.L., Smoller, J.W., Zöllei, L., Polimeni, J.R., Fischl, B., Liu, H., Buckner, R.L., 2011. The organization of the human cerebral cortex estimated by intrinsic functional connectivity. J. Neurophysiol. 106, 1125–65. doi:10.1152/jn.00338.2011

Zalesky, A., Fornito, A., Bullmore, E.T., 2010. Network-based statistic: identifying differences in brain networks. Neuroimage 53, 1197–207. doi:10.1016/j.neuroimage.2010.06.041

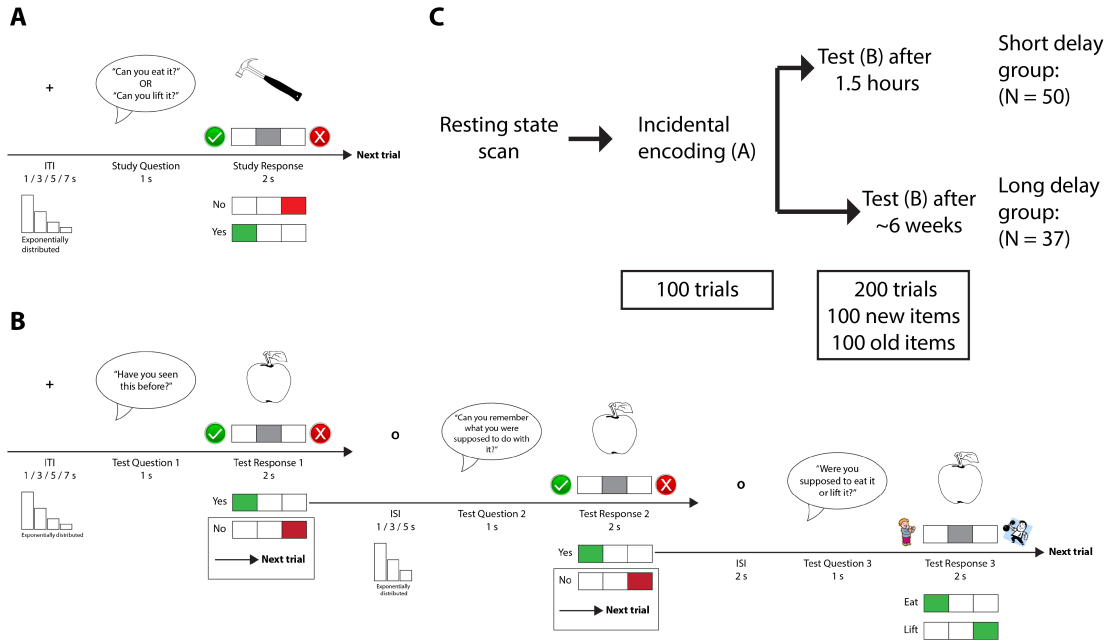

Figure 1

A) Encoding trial example. B) Test trial example. C) Design overview.

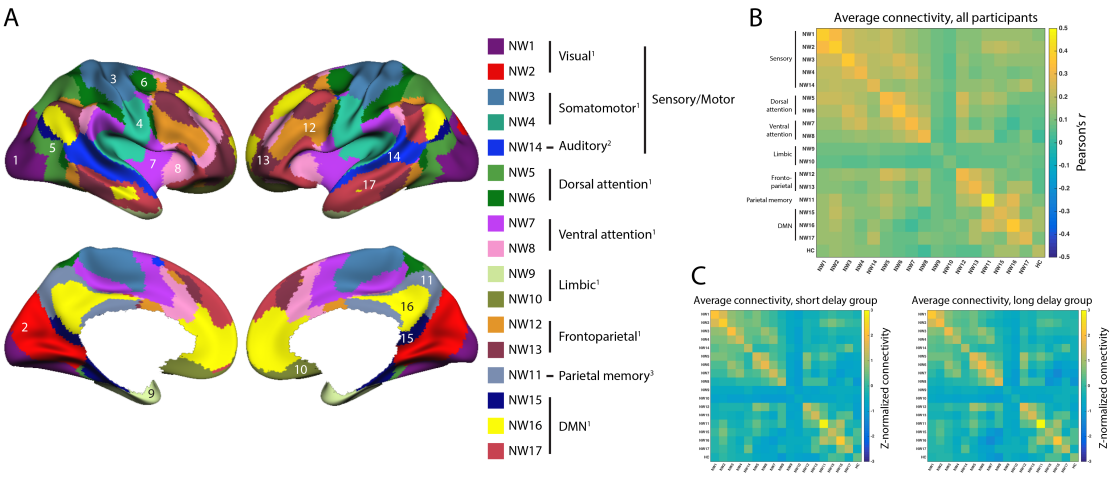

Figure 2

A) Summary of Yeo' 17-network cortical parcellation. [1]) Networks labeled by Yeo and colleagues (2011). Yeo et al. point out that the ventral attention networks (NW 7+8) likely encompasses networks often referred to in the literature as the salience (Seeley et al., 2007) or cingulo-opercular (Dosenbach et al., 2007) network. [2]) NW 14 which covers regions involved in auditory processing and perception (Rauschecker and Scott, 2009). [3]) NW 11 which recently has been singled out as a Parietal Memory Network involved in broad aspects of memory processing (Gilmore et al., 2015). B) Average connectivity within and between all investigated networks across all 87 participants in the study; individual connectivity matrices were r-to-z transformed following Fischer's method before being averaged. The presented average connectivity matrix is the resulting matrix following Fischer's z-to-r transformation. HC indicates hippocampal connectivity. C) Average connectivity within the two groups following standardization of each participant's Fischer r-to-z transformed connectivity matrix.

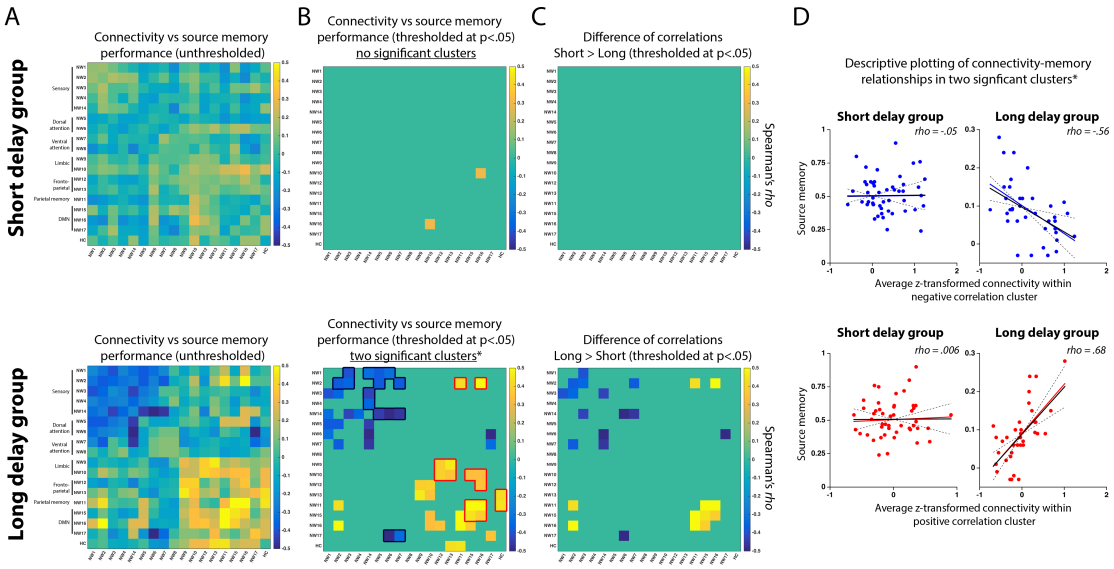

Figure 3

A) Spearman correlations between individual differences in corrected source memory estimates and rsFC, separated by group. B) Same as [A], but thresholded at a significance level of *p(rho)* < .05. Random permutation testing and cluster inference were run on these matrices. Two clusters of connected edges in the long delay group survived correction; one positive and one negative. The unique edges associated with these clusters are marked in red and black, respectively. No edges in the short delay group survived correction for multiple comparisons, either at a single-edge level or at a cluster level. C) Edges falling within the significant clusters and showing significantly different correlation strengths between the two groups at *p(difference of rho)* < .05. D) Scatter plots of the relationships between corrected source memory estimates and average connectivity within the two significant clusters in the long delay group. The plots are shown for descriptive purposes: blue/red opaque lines indicate the least squares relationship; black opaque lines indicate relationship following robust regression. Dashed lines indicate 95% confidence interval of the slope of the robust regression.

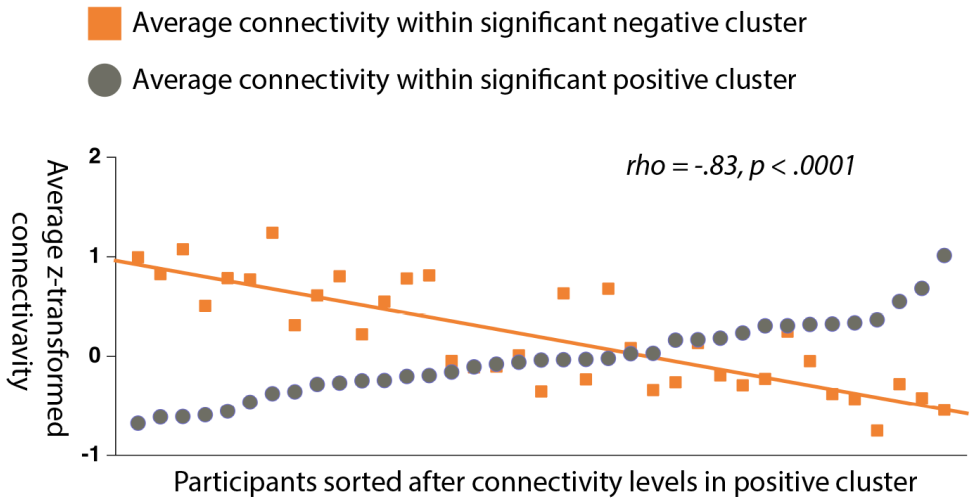

Figure 4

Average connectivity levels within the two significant clusters in the long delay group. The orange line shows the best fitting least squares slope of connectivity within the significant negative cluster across participants.

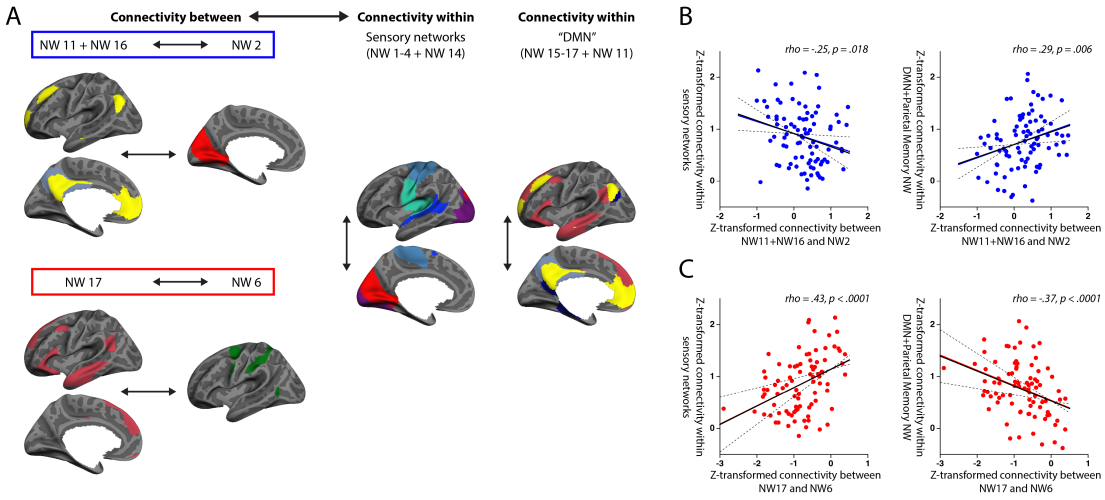

Figure 5

A) Three edges were found to connect the two clusters of networks shown to relate to long-term memory performance in Figure 3C. In the full sample of 87 participants we investigated the effect connectivity levels within these connecting edges has on connectivity within the "Sensory" network system and the "DMN". B-C) Scatter plots of connectivity within sensory networks and "DMN" against connectivity levels in the connecting edges. Black lines in scatter plots show results of robust regression and 95% confidence interval of the slope - for descriptive purposes. Uncorrected *p*-values associated with the correlations are presented above the scatter plots. Corrected values are reported in the text.

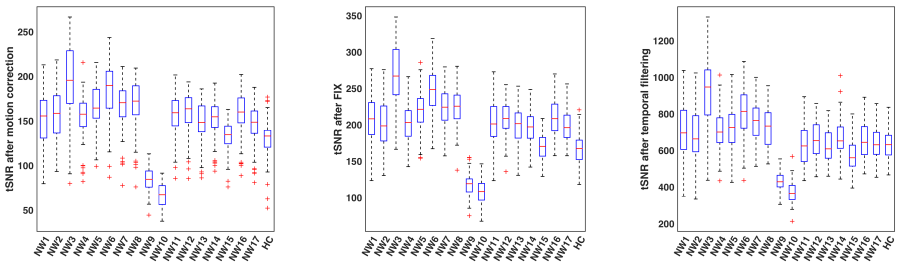

Supplementary Figure 1

Temporal signal-to-noise ratios (tSNR) of each network at different stages of preprocessing: following standard motion correction (left), following additional FIX-cleaning (middle), following additional temporal filtering (right).

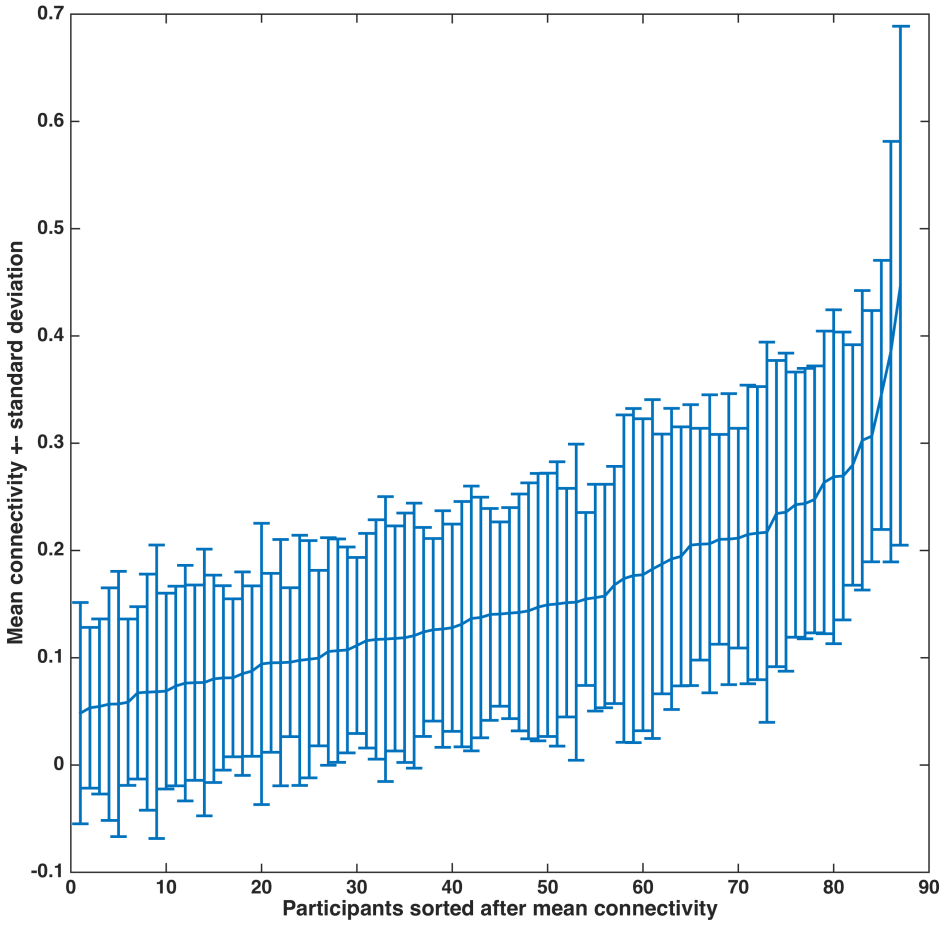

Supplementary Figure 2

Illustration of absolute connectivity differences between the 87 participants included in the study. Mean connectivity refers to the mean across each participant's network connectivity matrix (only unique edges included).

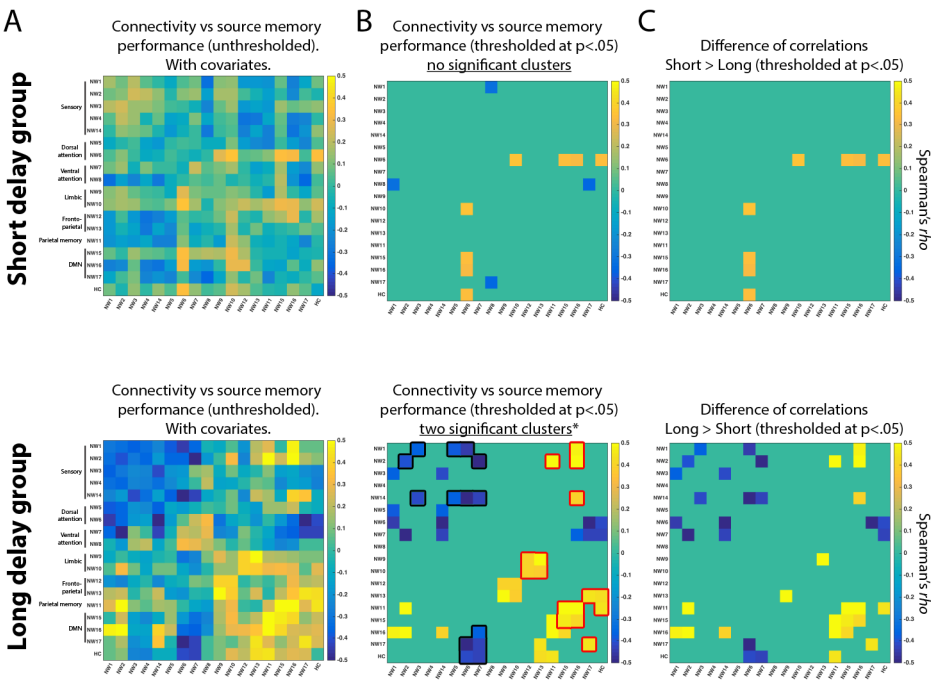

Supplementary Figure 3

Same as Figure 3 in the main text, but including covariates (IQ, digit span, delay interval in the long delay group). Significant positive cluster in long delay group: permuted p = .020. Significant negative cluster in long delay group: permuted p = .021.

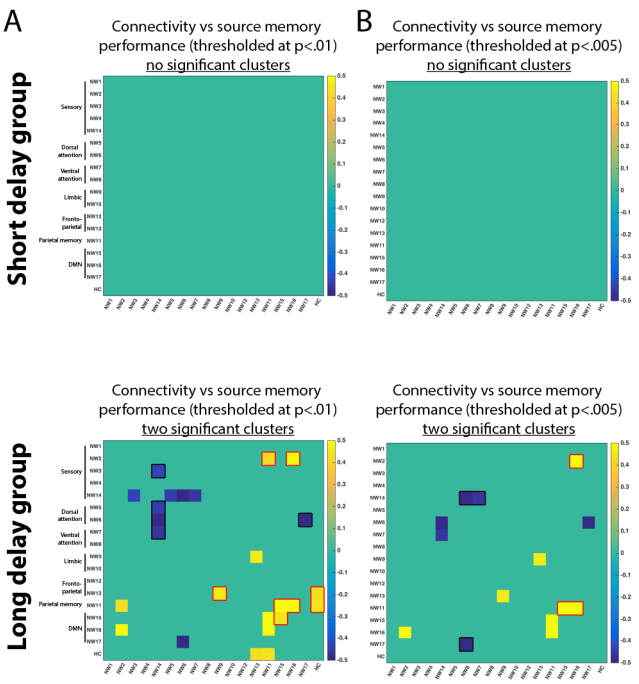

Supplementary Figure 4

Same as Figure 3B in the main text, but using alternative cluster-forming thresholds.

A) p < .01, corresponding to a rho of ±.36 in the short delay group and ±.42 in the long delay group. Significant positive cluster in long delay group at p < .01: permuted *p* = .006. Significant negative cluster in long delay group at p < .01: permuted *p* = .026.

B) p < .005, corresponding to a rho of ±.39 in the short delay group and ±.45 in the long delay group. Significant positive cluster in long delay group at p < .005: permuted *p* = .038. Significant negative cluster in long delay group at p < .005: permuted *p* = .039.

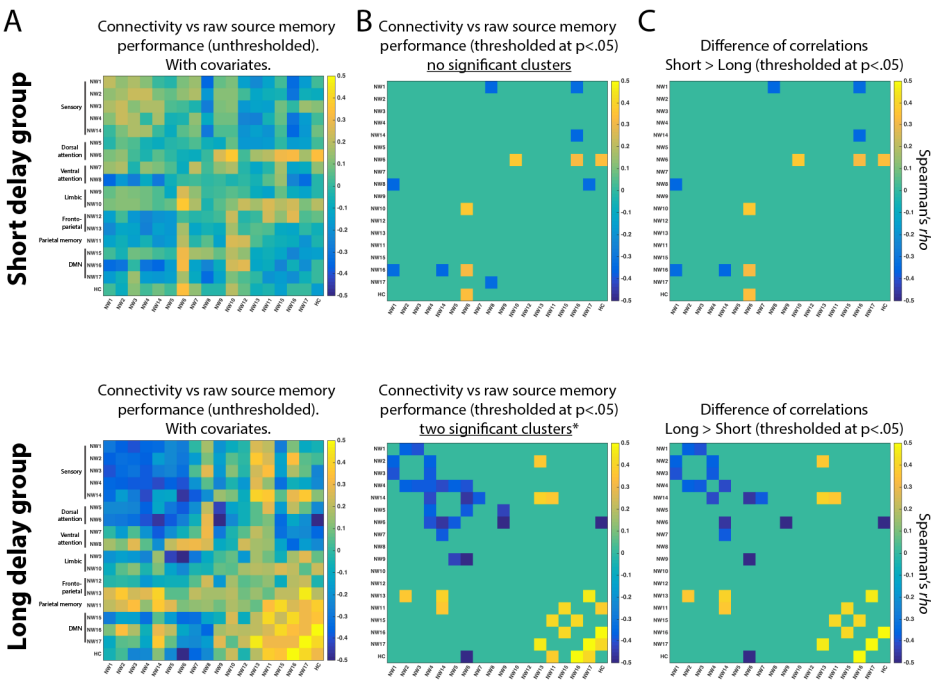

Supplementary Figure 5

Same as Figure 3 in the main text, but using uncorrected source memory scores as behavioral estimates. Significant positive cluster in long delay group: permuted p = .012. Significant negative cluster in long delay group: permuted p = .049.

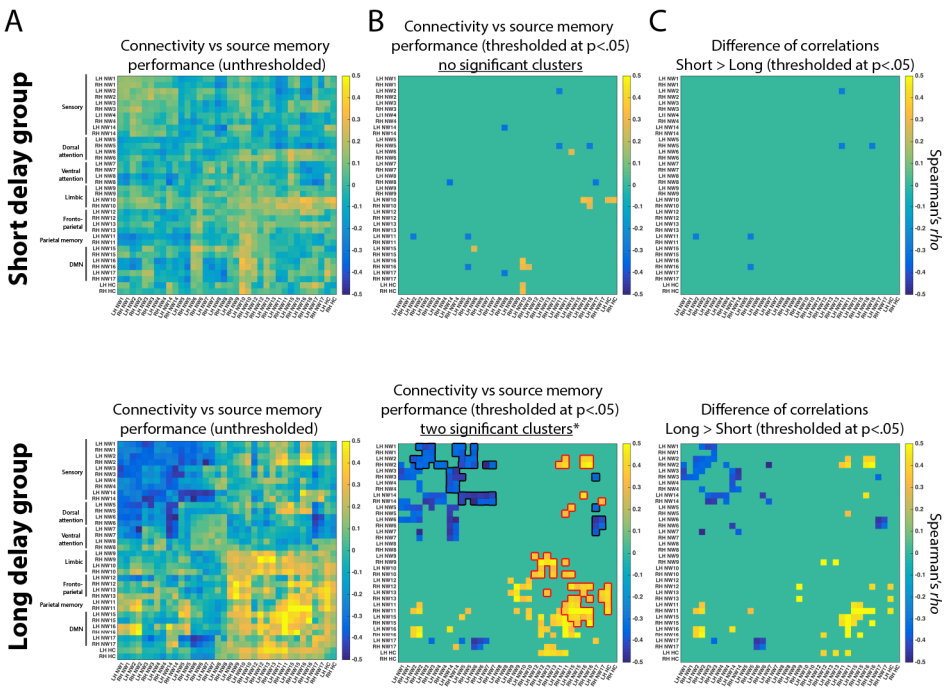

Supplementary Figure 6

Same as Figure 3 in the main text, but separating networks across hemispheres.

Significant positive cluster in long delay group: permuted p = .012. Significant negative cluster in long delay group: permuted p = .013.

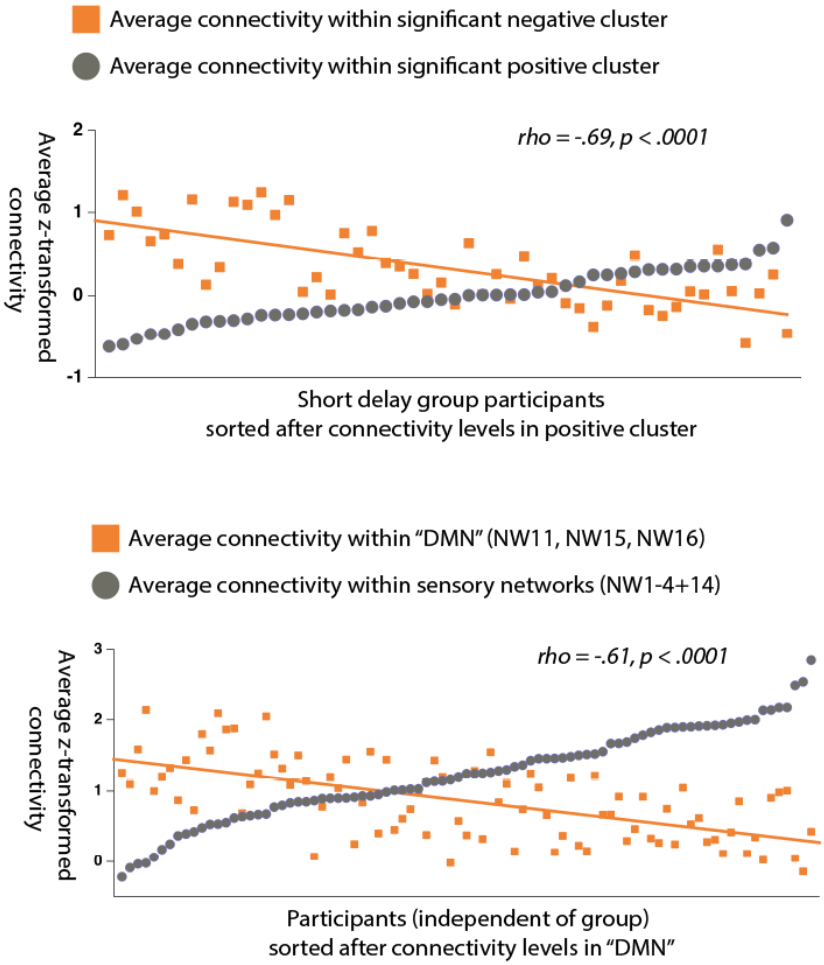

Supplementary Figure 7

Top panel: same plot as Figure 4 in the main text, but depicting data from the short delay group. Bottom panel: Plot of the negative correlation between individual differences in the "DMN" cluster and connectivity within the sensory networks. All 87 participants included.

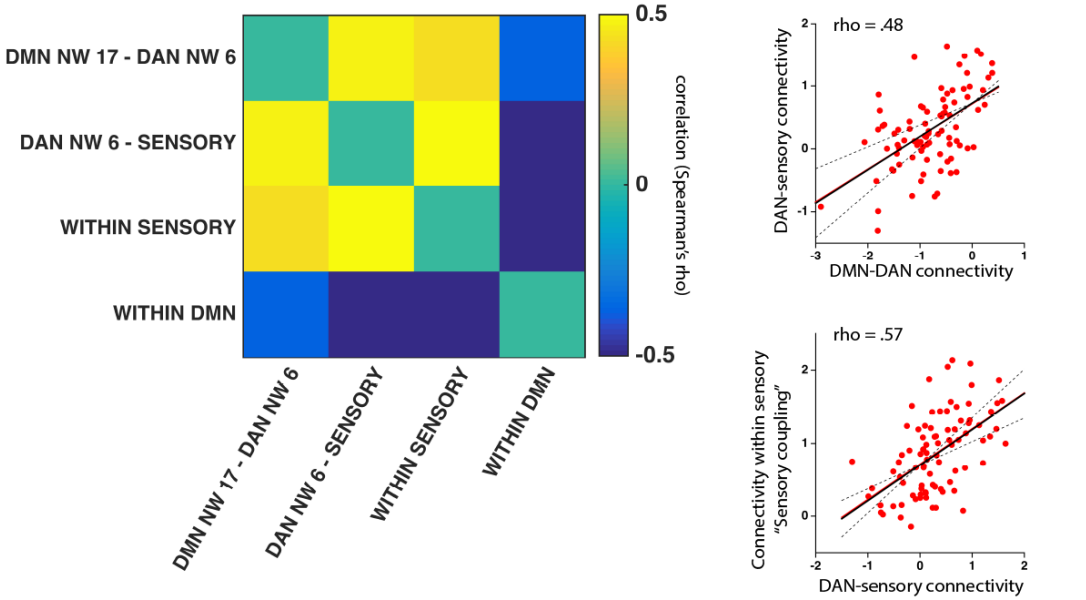

Supplementary Figure 8

Left panel: correlations (Spearman's rho) between DMN-DAN connectivity levels, DAN-sensory connectivity levels, and connectivity levels within sensory networks (NW1-4 + NW14) and "DMN" (NW15-17 + 11). All correlations were significant at the p<.05 level following Bonferroni correction for six tests. Right panel: scatter plots of two selected edges in the correlation plot.